MICROSTRUCTURE STUDIES ON A MG-AL-SI ALLOY (AS21X)

M. Cabibbo*, E. Evangelista, S. Spigarelli
INFM / Dipartimento di Meccanica, Università Politecnica delle Marche, Via Brecce Bianche, I-60131 Ancona, Italy

Abstract

The microstructure in a crept AS21X was investigated; β-$Mg_{17}Al_{12}$, Mg_2Si and β'-(Mn, Fe)(Al, Si) particles were observed alongside with extensive twinning and dislocation pile-ups against grain boundaries. Dislocations were basically confined to the slip planes: $\{0\bar{1}2\}\{0\bar{1}1\}$ and $\{0\bar{1}3\}$.

Keywords
Transmission Electron Microscopy, magnesium alloys, twinning, dislocations

Riassunto

Sono stati studiati i fenomeni microstrutturali alla base della risposta a creep di una lega di magnesio AS21X. In particolare, sono state osservate le due seconde fasi β-$Mg_{17}Al_{12}$ e Mg_2Si e l'intermetallico β'-(Mn,Fe)(Al,Si), oltre a diffusi geminati e impilagli di dislocazioni lungo i bordi di grano. Le dislocazioni giacevano ed erano confinate lungo i piani di scorrimento: $\{0\bar{1}2\}\{0\bar{1}1\}$ and $\{0\bar{1}3\}$.

Parole chiave
Microscopio elettronico in trasmissione, leghe di Magnesio, geminati, dislocazioni

INTRODUCTION

Light-weight magnesium alloys have attracted increasing interest in recent years for applications in the automotive, aircraft and electronic industries [1-4]. The limited ductility of Mg-alloys is basically due to their h.c.p. structure; significant development efforts are thus required to broaden their applicability. Susceptibility to intergranular stress-corrosion-cracking, which strongly depends on alloy composition and heat treatment, is another key drawback. A great deal of research has been addressed, for example, at studying dislocation pile-ups against grain boundaries in Al alloys, and the underlying mechanism has been used to predict susceptibility to stress-corrosion-cracking [5,6]. On the other hand, the attempt to improve the strength of Mg alloys and to develop new high-strength alloys has been limited by a lack of understanding of the structure, morphology, composition and distribution of both strengthening precipitate phases and of microstructural factors, like twinning, influencing and controlling the strength of Mg alloys. Twinning systems of types $\{0\bar{1}2\}\{0\bar{1}1\}$ and $\{0\bar{1}3\}$ were observed and referred to the c axis of the h.c.p. Mg lattice. Slip systems such as $\{1\bar{2}2\}\langle 10\bar{1}0\rangle$ were also present. Generally, twins formed by the c-axis are thin and do not contribute significantly to the material's ductility. In fact, the ductility of Mg alloys improves only at high temperatures, where the contribution of twinning becomes less important [7].

The creep resistance of conventional die-cast Mg-alloys is generally low, but the AS21 alloy, in particular, was found to exhibit an interesting creep strength up to 100°C. The precipitation of Si-rich phases in this alloy is held [8-9] to enhance long-term creep properties with respect to alloys containing only $Mg_{17}Al_{12}$ particles, which are more prone to coarsening. On the other hand, the standard AS21 exhibits lower corrosion resistance than AZ91D; nevertheless, an addition of Ce-rich mish metal (RE) in low-Mn AS21, leading to the new AS21X, resulted in much improved corrosion resistance compared to the conventional alloy [8]. In this paper, the second-phase precipitation, twinning mechanism, and dislocation arrangements of the creep-tested AS21X Mg-alloy were studied by means of energy dispersive spectrum (EDS) analysis by scanning electron microscopy (SEM) and transmission electron microscopy (TEM) techniques.

EXPERIMENTAL DETAILS

The chemical composition of the Mg-Al AS21X alloy is 2.1 Al, 0.94 Si, 0.16 Zn, 0.09Mn, 0.10 rare-earth, bal. Mg. For SEM investigations, specimens were polished and etched with a solution consisting of 10% HNO_3 in ethanol for a few seconds, then etched using a solution of 5 ml acetic acid, 6 g picric acid, 10 ml distilled water and 10 ml methyl alcohol. Thin foils for TEM analysis were prepared using a double-jet ion mill working at low temperature, an incident angle of 14°, and V = 5 V. A Philips XL30 scanning electron microscope equipped with EDS and back-scattered electron (BSE) signal, and a Philips CM200 transmission electron microscope equipped with a double-tilt specimen-holder and nano-probe microanalysis were used for microstructural studies. EDS analysis was performed in different regions of the specimen (within the grains, in grain boundaries and in second-phase particles); data come from statistical calculations made on the different regions analyzed. TEM inspections were carried out at 200 kV by tilting specimens so as to visualize the dislocation slip direction of the grains <120> parallel to the beam. A Siemens D5000 X-ray diffractometer equipped with Euler double-cradle was used to acquire the different diffraction peaks related to the secondary phases present in the material. Peak fitting and refinement were performed using a dedicated Bruker¨ software.

Constant-load creep tests were carried out in the temperature range between 120 and 180°C on specimens 30 mm in gauge length and 5 mm in diameter; sample elongation was continuously recorded during each test; most of the samples were pulled up to rupture.

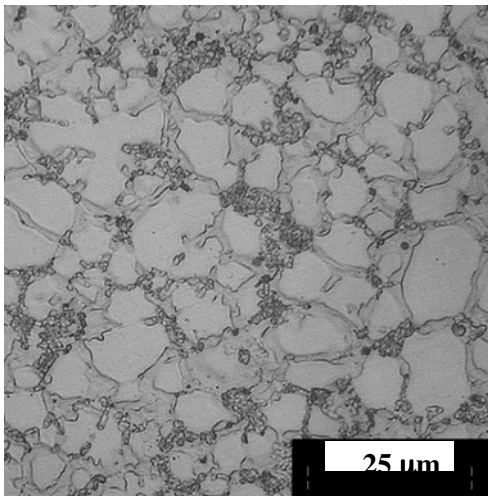

Fig. 1: Microstructure of the as die-cast AS21X alloy as observed in light microscopy; the structure consists of primary grains of magnesium-rich solid solution surrounded by Al-rich divorced eutectic. Occasionally very large grains can be observed; this grain morphology derives from the presence in the melt metal flowing in the die cavity of large and isolated solid "floating crystals".

RESULTS AND DISCUSSION

Figure 1 shows the microstructure of AS21X at low magnification (light microscopy). The grain interior consists of Mg-Al solid solution, with increasing Al content from the grain center to the boundaries [10]. In Al-rich grain boundary zones, there were particles with a variety of morphologies, from small particles to larger dendrites with the characteristic "Chinese Script" structure. The microstructure was decorated with second-phase particles both in the grain boundary and occasionally within the grains (Figure 2). In particular, several grain boundary needle-like particles were characterized by a lighter contrast than the rest of the microstructure. These early microstructure inspections and the Mg-Al-Mn phase diagram [11] allowed to identify the second phases as Mg_2Si and b ($Mg_{17}Al_{12}$) [10,12-21]; previous investigations at higher magnification revealed that rare-earth elements form phases with Si and with Mn [20], although previous detailed SEM and TEM analyses [21] unambiguously demonstrating that the predominant precipitated phase is Mg_2Si. X-ray diffraction measurements were carried out to verify the presence of other secondary phases containing the two remaining more abundant elements, Zn and Mn, not revealed by SEM (Table 1). A third phase, identified as b' (Mn,Fe)(Al,Si), was clearly detected by X-ray diffraction (see also [10]). Moreover, the higher peak intensity of the Mg_2Si phase compared with those of the β-$Mg_{17}Al_{12}$ confirms a more extensive presence

Table 1. Crystallographic directions of each detected peak referring to the different existing phases (Mg-matrix, Mg_2Si, b-$Mg_{17}Al_{12}$ and β'-(Mn,Fe)(Al,Si).

Mg	Mg_2Si	$Mg_{17}Al_{12}$	$(Mn_{4.6}Fe_{0.4})Si_3$
(00.2)	(112)	(721)	(410)
(10.1)	(202)	(660)	(004)
(10.2)	(210)	(510)	
(11.0)	(400)	(550)	
(10.3)			

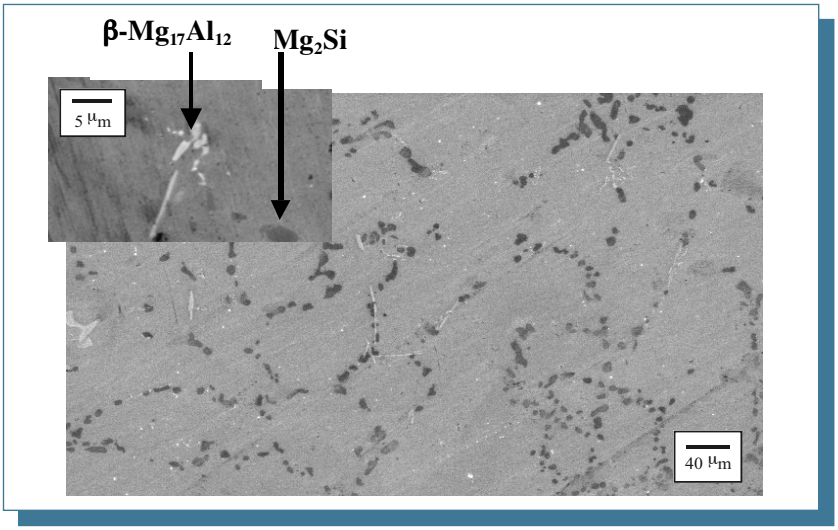

Fig. 2: Back-Scattering electron SEM image of the material; the inlet reports a detailed region showing the two different second phase particles: Mg $_2$Si and b-$Mg_{17}Al_{12}$.

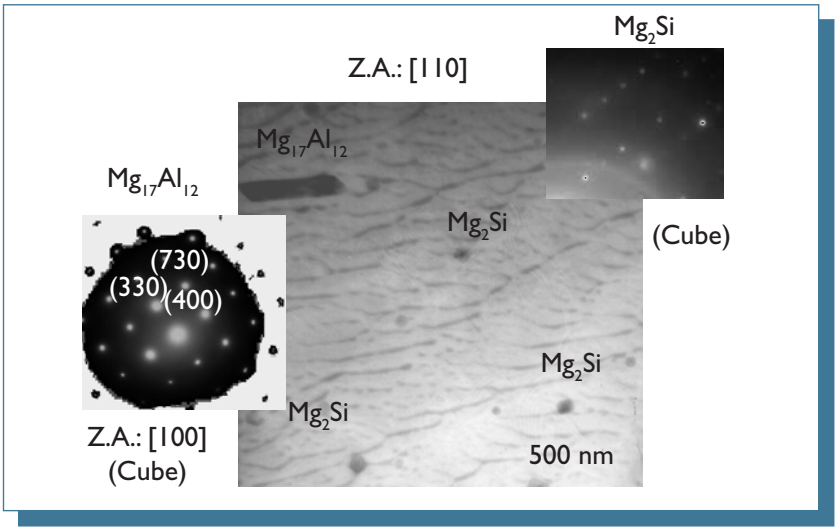

Fig. 3: TEM representative image showing the indexing and detection of Mg_2Si and $Mg_{17}Al_{12}$ secondary phase particles present in the microstructure's material. The related SAEDP, together with zone axis, are shown and indexed. Material after creep test.

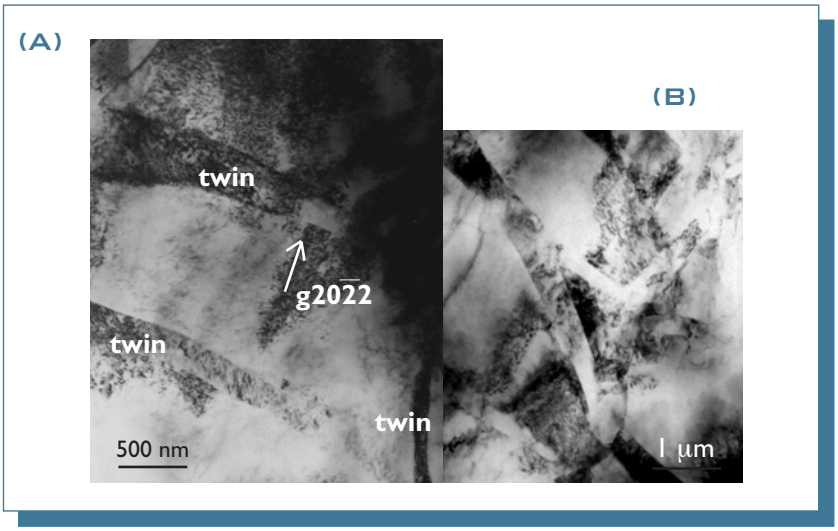

Fig. 4: a) Representative BF-TEM image showing the abundant presence of twins in the microstructure of the material after creep test (g = [2022]); b) Representative BF-TEM image showing two twins in which the ending of one corresponds to the beginning of the second one.

of the Si-rich than the Al-rich phase. All the above mentioned and detected secondary phases were identified by transmission electron microscopy techniques coupled with selected area electron diffraction pattern (SAEDP) and a representative image is reported in Figure 3.

The creep curves obtained by testing under constant load the as-cast AS21X alloy exhibit a conventional shape, with a pronounced primary stage (particularly in the high-stress regime), a minimum creep rate range, and a prolonged tertiary stage (for a more detailed description of creep data, see [9, 22]). The microstructure of the sample crept at 180°C-100 MPa, at low magnification (LM), is still substantially similar to that shown in Figure 1.

TEM analysis showed that an extensive presence of twins is a common feature in both as-received and crept conditions. Thin twins, often grouped in parallel bundles with other intersecting, within single grains, were extremely common (Figure 4). In general, the twins terminated with sharp boundaries next to the grain boundary, but occasionally they extended through it, causing boundary deflection and distortion. Twinning is held to occur within grains poorly oriented for slip, producing more favored orientations for basal slip and enhancing multiple slip [23-25]. Most of the twins observed were of $\{10\bar{1}2\}$ type. After creep at 180°C, most twins assumed a lenticular shape and frontal growth of the plates occurred, contributing to their spreading across the grain. It can be hypothesized that the crept material presented a splitting of twins from the original to double twinning; these thin new twins have also been found in Mg alloys deformed in the same range of testing temperatures in grains unfavorably oriented for basal slip [26].

In some cases, twins appeared as narrow bundles that occasionally encroached on one another; in other cases, they were in form of thick lenses with curved boundaries. SAED pattern revealed twin boundary misorientation with respect to the grain to be typically ~4° (Figure 5). Within twins, some dislocations lying on slip planes and others in tangles were detected; an inner substructure often decorated the twin interior (Figure 5 (a),(b)). Moreover, secondary phase particles were also detected inside twins (Fig. 5 (a)). The role of twinning in the deformation of h.c.p. lattice alloys is well known [25]; in addition, twinning can also favor the formation of new grain structure, and indeed new fine grains separated by high-angle

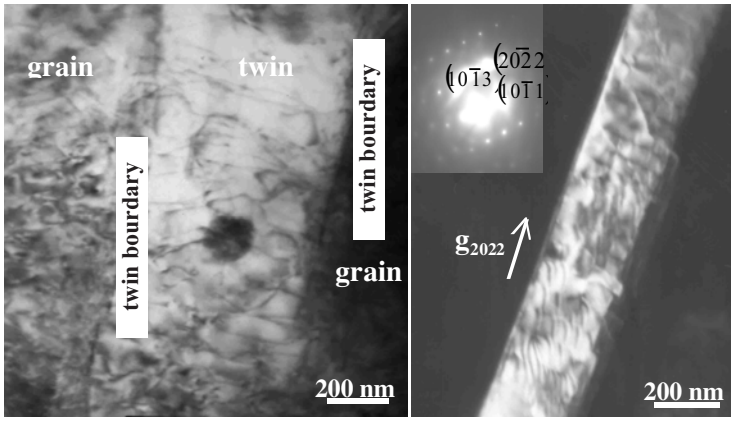

Fig. 5: a) BF-TEM image showing the interior of a twin decorated by arrays of dislocations resembling low-angle boundary subgrains, a secondary phase particle is also present within the two twinning boundaries; b) DF-TEM showing a twin interior structure (g = []).

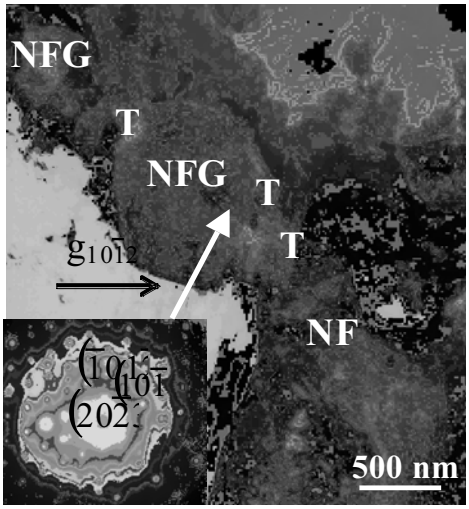

Fig. 6: BF-TEM image showing a new fine grain (NFG) structure having high-angle boundaries in correspondence of twins (T) (g = []). The SAED pattern of a NFG superimposing a T is also reported, it shows a little angular mismatch across the NFG-T boundary.

boundaries had developed, and were documented, in correspondence of twins within the grain (Figure 6). The authors believe the formation of these high-angle boundaries to be produced by twin-twin intersections. The non-basal dislocation slip toward the basal slip dislocations of the twins could be co-responsible for the formation of non-equilibrium new grain boundaries. Studies [26-28] reporting the presence of several internal stress fields generated by the new grain with non-equilibrium boundaries appear to support this view.

CONCLUSIONS

Creep tests of an AS21X magnesium alloy were carried out at 100MPa / 180°C. EDS analysis allowed to detect the two most abundant second-phase particles: β-$Mg_{17}Al_{12}$ and Mg_2Si. A minor amount of a third phase, β'-(Mn,Fe)(Al,Si), was also detected using X-ray diffraction techniques.
Twinning systems operating in the crept alloy microstructure and dislocation slip systems together with their pile-up mechanism were detected and studied. Twins were sometimes grouped into narrow, parallel bundles and in other cases they were thick lenses with curved boundaries. Lattice rotation in high-density dislocation regions next to twin boundaries resulted in the formation of fine new grains characterized by non-equilibrium boundaries. Such grain formation is typical of low-temperature plastic deformation and of the creep response to microstructure deformation mechanisms of magnesium alloys.

ACKNOWLEDGMENT

The authors are grateful to Mr. D. Ciccarelli for his help in preparing the specimens for LM and SEM inspections.

REFERENCES

[1] J.F. Nie, "Precipitation and Strengthening in selected magnesium alloys", Magnesium Technology 2002, TMS, Ed. H.I. Kaplan, 2002, 103.

[2] W. Blum, P. Zhang, B. Watzinger, B.v. Grossmann and H.G. Haldenwanger, "Comparative study of creep of the die-cast Mg-alloys AZ91, AS21, AS41, AM60 and AE42", Mater. Sci. Eng., A319-321, 2001, 735.

[3] A.A. Luo, "Materials comparison and potential applications of magnesium in automobiles", Magnesium Technology 2000, TMS, Ed. H.I. Kaplan, J. Hryn, and B. Clow, 2000, 89.

[4] B.L. Mordike and T. Ebert, "Magnesum:Properties, Applications, Potential", Mat. Sci. Eng., A302, 2001, 37.

[5] M.O. Speidel, Proc. Int.l Conf. On Fundamental Aspects of Stress Corrosion Cracking, Ed. R.W. Staehle, A.J. Forty, D. Van Royen, 1967, 561.

[6] R.M. Wang, A. Eliezer and E. Gutman, "Microstructures and dislocations in the stressed AZ91D magnesium alloy", Mater. Sci. Eng., A344, 2002, 279.

[7] O.D. Sherby and E.M. Taleff, "Influence of grain size, solute atoms and second-phase particles on creep behavior of polycrystalline solids", Mat. Sci. Eng., A322, 1-2, 2002, 89.

[8] B.L. Mordike, "Creep-resistant magnesium alloys", Mat. Sci. Eng., A324, 1-2, 2002, 103.

[9] N.E. Paton and W.A. Backofen, Met. Trans., 1, 1970, 2839.

[10] B. Bronfin, M. Katsir and E. Aghion, "Preparation and solidification features of AS21 magnesium alloy", Mater. Sci. Eng., A302, 2001, 46.

[11] D.R.F. West, N. Saunders, Ternary phase diagrams in Materials Science, Maney Publisher, New York, 2002.

[12] I.J. Polmear, "Physical Metallurgy of Magnesium Alloys", Magnesium and Magnesium Alloys, Pergamon Press, 1977, 201.

[13] J.F. Nie, X.L. Xiao, C.P. Luo, and B.C. Muddle, "Characterisation of precipitate phases in magnesium alloys using electron microdiffraction", Micron, 32, 2001, 857.

[14] A. Mwembela, E.B. Konopleva, and H.J. McQueen, "Microstructural development in Mg alloy AZ31 during hot working", Scripta Metall. Mater., 37, 11, 1997, 1789.

[15] A. Bussiba, A. Ben Artzy, A. Shtechman, S. Ifergan, M. Kupiec, "Grain refinement of AZ31 and ZK60 Mg alloys, towards superplasticity studies", Mat. Sci. Eng., A302, 2001, 56.

[16] Y.C. Lee, A.K. Dahle, and D.H. StJohn, "Grain refinement of magnesium", Magnesium Technology 2000, Ed. H.I. Kaplan, and B. Clow, 2000, 211.

[17] R. Ninomiya, T. Ojiro, and K. Kubota, "Improved heat resistance of Mg-Al alloys by the Ca addition", Acta Metall. Mater., 43, 2, 1995, 669.

[18] D. Duly, M. Audier, and Y. Brechet, "On the influence of plastic deformation on discontinuous precipitation in Mg-Al", Scripta Metall. Mater., 29, 1993, 1593.

[19] C.H. Caceres, C.J. Davidson, J.R. Griffiths, and C.L. Newton, "Effects of solidification rate and ageing on the microstructure and mechanical properties of AZ91 alloy", Mat. Sci. Eng., A325, 2002, 344.

[20] M. Avedesian, H.B. Hardbound (Eds.), Magnesium and Magnesium Alloys, ASM, New York; 1998.

[21] G. Pettersen, R. H¿ier, O. Lohne and H. Westengen, "Microstructure of a pressure die cast magnesium 4wt.% aluminium alloy modified with rare earth additions", Mater. Sci. Eng., A207, 1996, 115.

[22] E. Gariboldi and S. Spigarelli, "An analysis of strain–time relationships for creep in an as-cast Mg–Al–Si alloy", Mater. Design, 24, 6, 2003, 445.

[23] M. Loreth, J. Morton, K. Jacobson, F. Katrak and J. Agarwal, Proc. Met. Soc. CIM, Recent Metallurgical Advances in Light Metals, Ed.: S. MacEwan, J.P. Gilardeau, 1995, 11.

[24] C.S. Roberts, Magnesium and its Alloys, Wiley, New-York, 1960, 154.

[25] S.E. Ion, F.J. Humphreys and S.H. White, " Dynamic Recrystallization and the development of microstructure during the hugh temperature deformation of magnesium", Acta Met., 30, 1982, 1909.

[26] B.C. Wonseiwicz and W.A. Backofen, Trans. Am. Inst. Min. Metals, 239, 1967, 1422.

[27] R.Z. Valiev, A.N. Vergazov and V.Y. Gertsman, "Crystallogeometric analysis of intercrystalline boundaries in the practice of Electron Microscopy, Moscow-Nauka, 1991, 63.

[28] A. Belyakov, T. Sakai, H. Miura and R. Kaibyshev, Strain induced submicrocrystalline grains developed in austenitic stainless steel under severe warm deformation", Phil. Mag. Lett., 80, 2000, 711.